

Synthesis of Porous Wires from Directed Assemblies of Nanospheres

Feng Li,^{†,‡} Jibao He,[‡] Weilie L. Zhou,[‡] and John B. Wiley^{*,†,‡}

Department of Chemistry and the Advanced Materials Research Institute, University of New Orleans,
New Orleans, Louisiana 70148-2820

Received September 10, 2003; E-mail: jwiley@uno.edu

Recent efforts have produced significant advances in the fabrication of one-dimensional nanostructures. A variety of methods have been described for the production of wires,^{1–6} ribbons,⁷ corrugated wires,⁸ helical wires,⁹ tubules,¹⁰ etc. Further efforts have been directed toward the development of technologies based on these components: studies on electronic, magnetic, optical, and sensor materials, for example, have been reported.^{11–14} Most of this work has involved solid nanowires^{1–3} or superlattice structures.^{15–17} Relatively few studies have examined control of spatial variation along or within wires.^{4–6} Such control could impact properties, especially those important to sensor, catalytic, and optical applications. Herein we report the preparation of porous wires. The use of template methods is well-known for growing wires. By infiltrating porous membranes with nanoscale spheres, we can modify these templates so that they allow the production of wires with extended pore structures.

The general procedure used to fabricate porous wires is shown in Figure 1. Initially, two porous membranes with different channel diameters are placed flush to each other. Spheres are infiltrated into the upper membrane by vacuum filtration with the membrane pore size differences (ca. 10 \times) helping to lock them in place. The membrane–sphere composite is converted to an electrode for deposition of gold or nickel metal.¹⁸ Finally, the membrane and spheres are dissolved to produce porous wires.

Porous wires can be grown from anodized alumina (AAM) or polycarbonate (PCM) membranes containing either silica or polystyrene (PS) spheres. Figure 2 shows wires produced from PCM (1- μ m channels) and silica spheres. Spheres (500-nm) in and out of the channels can be observed prior to the growth of the porous wires (Figure 2a). Electrodeposition within the modified membranes readily produces porous gold wires. Varying the size of the spheres allows one to control the pore size within the wires. Figure 2b–d and 2e,f present micrographs of porous wires arrays made from 500- and 300-nm silica spheres, respectively. Evidence for extended pore structures can be seen along the length and tips of the wires as well as from cross section images (insets Figures 2b,f). The arrangement of the spheres in the membrane channels dictates the pore structure in the wires. Contacts between the spheres and the channel wall result in pores on the surface of the wires, and contacts between the spheres themselves produce openings between adjacent pores.

Smaller pore nickel and gold wires, prepared from 300-nm channel alumina templates and 140-nm silica spheres, are presented in Figure 3. Arrays of these wires are obtained after removal of the alumina and silica components (Figure 3a). While most of the wire surfaces show extensive pore structures, smooth surfaces are occasionally observed, indicating that the wire is either solid in these regions or that the pores do not penetrate to the surface. TEM

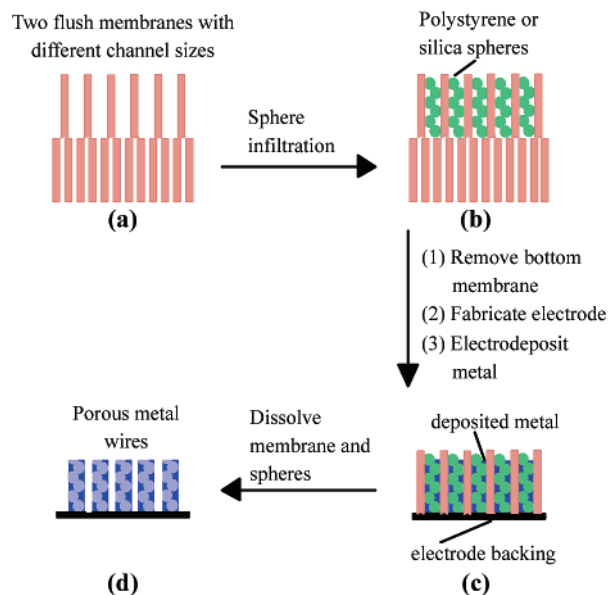


Figure 1. Fabrication of porous wires: (a) two flush, porous membranes with different channel diameters are (b) infiltrated with spheres. (c) After removing the bottom membrane, the top membrane is converted to an electrode, and metal is deposited within the void space. (d) The membrane and the spheres are dissolved to produce porous metal wires.

images (Figure 3b,c) of individual porous gold wires show interconnects between adjacent pores across the width of the wires.

The diameter of the spheres (d_s) relative to the membrane channels (d_c) can greatly influence sphere packing. In the simple case where the sphere diameters are close to those of the channels ($d_c = xd_s$, $x \approx 1$), simple linear packing is expected. As channels become slightly larger relative to spheres, a zigzag packing pattern is likely.¹⁹ At certain higher values of x (2 and 2.15), symmetric hexagonal close-packing-like (hcp) structures occur with a base consisting of two or three spheres. Other symmetric packings may be seen at specific x values where four, five, and seven spheres form a base, and subsequently, sets of equivalent layers can order above each other after rotations of 45°, 36°, and 30°, respectively.²⁰ Intermediate to these more symmetric (achiral) packings, chiral assemblies, either left- or right-handed, are possible, where helices (double, triple, quadruple, etc.) can form. Another symmetric, less efficient packing can also occur at $x = 2.22$ where two pairs of linear chains of spheres run parallel to the channel wall, with adjacent chains displaced by $d_s/2$.²⁰

The porous wires reported here exhibit a variety of packing geometries. In most instances, they deviate from the ideal, long-range packings described above. In the system prepared from PCM with 1- μ m channels and 500-nm spheres (i.e., $x = 2$), one might expect simple hcp-like packing. The PCM channel diameters, however, vary in size (Figure 2a), and consequently, the packings are varied. Further, packing faults appear quite common, likely due

[†] Department of Chemistry.

[‡] Advanced Materials Research Institute.

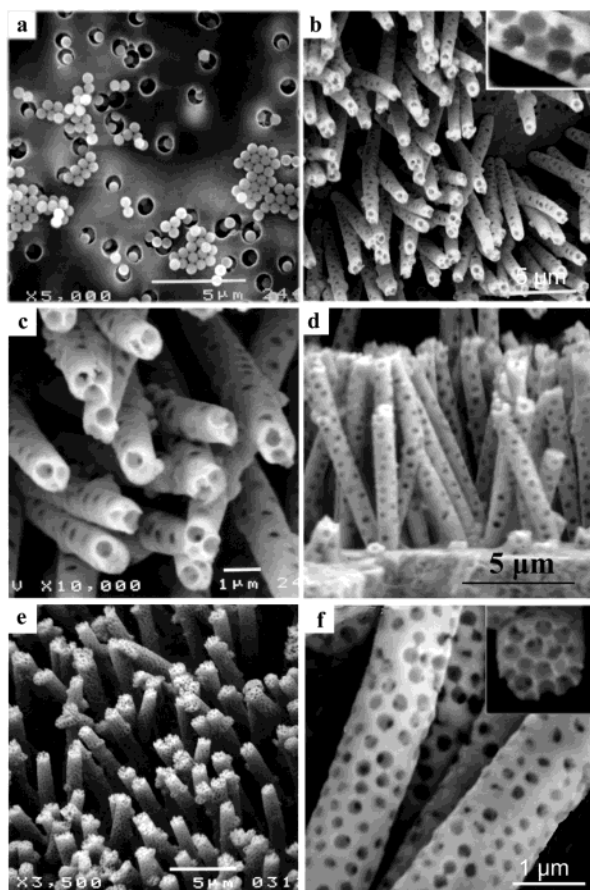


Figure 2. SEMs of (a) polycarbonate membrane with 500-nm SiO₂ beads and (b, c) top view and (d) side view of porous Au wire arrays with 500-nm pores. Inset in (b): Cross section along the length of a wire. (e) Top view and (f) side view of porous Au wires with 300-nm pores. Inset in (f): Cross section along width of 300-nm pore wire.

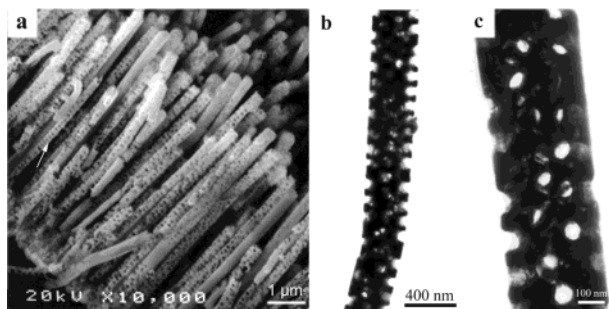


Figure 3. (a) SEM image of an array of 300-nm porous Ni wires with 140-nm pores and (b, c) TEM images of porous Au wires with 140-nm pores.

to the rapid infiltration of spheres. Some ordered regions are still observed as pores either along the surface of a wire or within cross sections. Zigzag packing for example is seen (inset, Figure 2b); this packing structure is consistent with a channel diameter smaller than twice the sphere diameter ($x \approx 1.87$). As the relative channel size increases ($1.87 < x < 2$, $2 < x < 2.15$),¹⁹ chiral packings could be expected; the arrangement of pores along the surface of several wires gives some indication of this, though packing defects or simply random arrangements of spheres are apparent (Figure 2b–d). On further increase of the relative channel size ($x > 3$, Figure 2e,f), short-range order packings predominate. In wires prepared from 140-nm spheres and 300-nm AAM ($x \approx 2.14$, Figure 3), similar levels of order occur, though evidence for the less

efficient, achiral packing ($x = 2.22$) is observed as a series of adjacent pores, especially clear along the right edge of the wire (Figure 3b).

The extensive pore structures of the wires will impact their physical properties. In terms of porosity and surface area, one can estimate these values by simple geometric considerations. If we assume nearly ideal packing²⁰ in, for example, the 1- μm wires with 300-nm spheres, we can estimate the porosity (% void volume) to be about 70% and the relative increase in surface area versus a solid wire to be about 4 times. The short-range order predominating in these systems would, however, work to lower these values slightly. In terms of strength, the pore structures decrease the mechanical strength of the wires where the smaller wires (Figure 3a) were found to be especially fragile.

The process presented here offers an effective method for the formation of porous wires. While samples were prepared by electrodeposition of Au and Ni, a variety of other elements and compounds, formed either chemically or electrochemically, could be fabricated into porous wires. These various structured materials could be used for applications in catalysis, electrolysis, and sensor arrays (e.g., hydrogen sensors); higher surface areas should serve to increase reactivity and sensitivity, and also, control of the pore morphologies might impact selectivity in chemical conversions. A further application for such materials might come in the form of photonic wires. While the rapid infiltration of spheres into the pores impeded the formation of the highly ordered structures desired in photonics, sphere precipitation into membrane channels over extended periods should lead to more order. Such wires could offer interesting properties, and the prospect of photonic wires, especially those based on helical packings, is particularly intriguing.

Acknowledgment. NSF-EPSCoR support, NSF/LEQSF (2001-04)-R11-03, is gratefully acknowledged. We thank R. Baughman and A. Zakhidov for helpful discussions.

Supporting Information Available: Detailed description of experimental procedures (PDF). This material is available free of charge via the Internet at <http://pubs.acs.org>.

References

- Xia, Y.; Yang, P.; Sun, Y.; Wu, Y.; Mayers, B.; Gates, B.; Yin, Y.; Kim, F.; Yan, H. *Adv. Mater.* **2003**, *15*, 353.
- Prieto, A. L.; Martin-González, M.; Keyani, J.; Gronsky, R.; Sands, T.; Stacy, A. M. *J. Am. Chem. Soc.* **2003**, *123*, 7160.
- Lauhon, L. J.; Gudiksen, M. S.; Wang, D.; Lieber, C. M. *Nature* **2002**, *420*, 57.
- Jung, J. H.; Kobayashi, H.; van Bommel, K. J.; Shinkai, C. S.; Shimizu, T. *Chem. Mater.* **2002**, *14*, 1445.
- Lou, X. W.; Zeng, H. C. *J. Am. Chem. Soc.* **2003**, *125*, 2697.
- Caruso, R. A.; Schattka, J. H.; Greiner, A. *Adv. Mater.* **2001**, *13*, 1577.
- Pan, Z. W.; Dai, Z. R.; Wang, Z. L. *Science* **2001**, *291*, 1947.
- Li, F.; Xu, L.; Zhou, W.; He, J.; Zakhidov, A. A.; Baughman, R. H.; Wiley, J. B. *Adv. Mater.* **2002**, *14*, 1528.
- Zhang, H.-F.; Wang, C.-M.; Wang, L.-S. *Nano Lett.* **2002**, *2*, 941.
- Kobayashi, S.; Hamasaki, N.; Suzuki, M.; Kimura, M.; Shirai, H.; Hanabusa, K. *J. Am. Chem. Soc.* **2002**, *124*, 6550.
- Mbindyo, J.; Mallouk, T. E.; Mattzela, J. B.; Kratochvilova, I.; Razavi, B.; Jackson, T. N.; Mayer, T. S. *J. Am. Chem. Soc.* **2002**, *124*, 4020.
- Thurn-Albercht, T.; Schotter, J.; Kastle, G. A.; Emley, N.; Shibauchi, T.; Krusin-Elbaum, L.; Guarini, K.; Black, C. T.; Tuominen, M. T.; Russell, T. P. *Science* **2000**, *290*, 2126.
- Huang, M. H.; Mao, S.; Feick, H.; Yan, H.; Wu, Y.; Kind, H.; Weber, E.; Russo, R.; Yang, P. *Science* **2001**, *292*, 1897.
- Cui, Y.; Wei, Q.; Park, H.; Lieber, C. M. *Science* **2001**, *293*, 1289.
- Li, Q.; Wang, C. *J. Am. Chem. Soc.* **2003**, *125*, 9892.
- Gudiksen, M. S.; Lauhon, L. J.; Wang, J.; Smith, D. C.; Lieber, C. M. *Nature* **2002**, *415*, 617.
- Wu, Y.; Fan, R.; Yang, P. *Nano Lett.* **2002**, *2*, 83.
- Xu, L.; Zhou, W. L.; Frommen, C.; Baughman, R. H.; Zakhidov, A. A.; Malkinski, L.; Wang, J.; Wiley, J. B. *Chem. Commun.* **2000**, 997.
- Pickett, G.; Gross, M.; Okuyama, H. *Phys. Rev. Lett.* **2000**, *85*, 3652.
- Erickson, R. O. *Science* **1973**, *181*, 705.

JA038452+